HHS Public Access

Author manuscript

J Org Chem. Author manuscript; available in PMC 2019 April 02.

Published in final edited form as:

J Org Chem. 2018 February 02; 83(3): 1278–1286. doi:10.1021/acs.joc.7b02813.

Six Trikentrin-like Cyclopentanoindoles from *Trikentrion flabelliforme*. Absolute Structural Assignment by NMR and ECD

Mariam N. Salib[†] and **Tadeusz F. Molinski**[*,†,§]

[†]Department of Chemistry and Biochemistry, University of California, San Diego, 9500 Gilman Dr. MC-0358, La Jolla, California 92093-0358.

[§]Skaggs School of Pharmacy and Pharmaceutical Sciences, University of California, San Diego, 9500 Gilman Dr. MC-0358, La Jolla, California 92093-0358.

Abstract

Six new cyclopenta[*g*]indoles were isolated from a West Australian sponge, *Trikentrion flabelliforme* Hentschel, 1912 and their structures elucidated by integrated spectroscopic analysis. The compounds are analogs of previously described trikentrins, herbindoles and trikentramides from related Axinellid sponges. The assignment of absolute configuration of the new compounds was carried out largely by comparative analysis of specific rotation, calculated and measured ECD and exploiting van't Hoff's principle of optical superposition. Five of the new compounds were chemically interconverted to establish their stereochemical relationships, leading to a simple chiroptical mnemonic for assignment of the this family of chiral indoles. The first biosynthetic hypothesis is advanced to explain the origin of the trikentrin-herbinole family, and proposes a pyrrole-carboxylic thioester initiated polyketide synthase mechanism.

Graphic Abstract

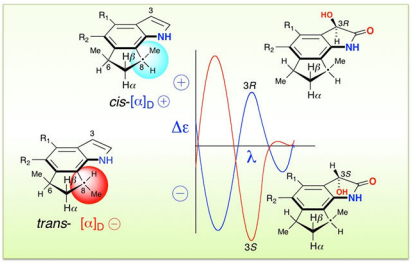

Introduction

The majority of marine indole alkaloids are derived from secondary metabolism of tryptophan. The indigo derivative, 'Tyrian purple' (6,6'-dibromoindigotin), from the hypobranchial gland of various marine mollusks, has been known since ancient times:[1]

[*]To whom correspondence should be addressed: Tel: +1 (858) 534-7115. Fax: +1 (858) 822-0386. tmolinski@ucsd.edu.

Supporting Information. CD spectra of (*S*)- and (*R*)-**19**, FTIR, ^{1}H, ^{13}C NMR and 2D NMR spectra of **13**–**18**, DFT calculations of *ent*-**6** and **13** (summaries and connection tables), ^{1}H NMR simulation of the H-8 multiplet of **13** and molar rotations, $[\phi]_D$, for **1**-**9**, and **11**-**18** The Supporting Information is available free of charge on the ACS Publications website at DOI: xxx

contemporary studies revealed its structure through X-ray crystallography.[2] Still more rare are simple indoles that lack carbon substitution at C-3; their structures imply biosyntheses that diverge substantially from tryptophan metabolism. In a study by Brennan and Erickson, one of the first investigations of red algae, 10 achiral polyhalogenated indoles were reported from *Rhodophyllis membranacea* Harvey, and more recent studies of *R. membranacea* have delivered another 18 new analogs.[3]

Among the more curious natural indoles are unique, optically active cyclopenta[*g*]indoles from two Axinellid sponges. Capon and MacLeod described antibacterial (+)-*cis*- and (+)-*trans*-trikentrins A (**1**, **2**), (–)-*trans*-trikentrin B (**4**) and an inseparable mixture of *cis*- and iso-*trans*-trikentrin B (**3** and **5**, respectively) from *Trikentrion flabelliforme* Hentschel, 1912, collected in Darwin, Australia.[4] Scheuer and coworkers characterized the trikentrin homologs, (–)-herbindoles A-C (**6**–**8**), from a specimen of *Axinella* sp. collected in Exmouth Gulf, Western Australia.[5] The latter compounds, which exhibit modest cytotoxicity and fish antifeedant activity, are antipodal in configuration to the *cis*-trikentrins as established through independent total syntheses of *ent*-(–)-**1**, (+)-**2**,[6] and *ent*-(+)-**6**–**8** by Natsume and coworkers,[7] and of (+)-**4** by Kanematsu and coworkers.[8] (+)-Trikentramides A-D (**9**–**12**), isolated and characterized by Quinn and coworkers from a specimen of *T. flabelliforme* collected at Port Hedland (500 km from Exmouth), are isatin and oxindole analogs of (+)-*cis*- and (+)-*trans*-trikentrins A.[9]

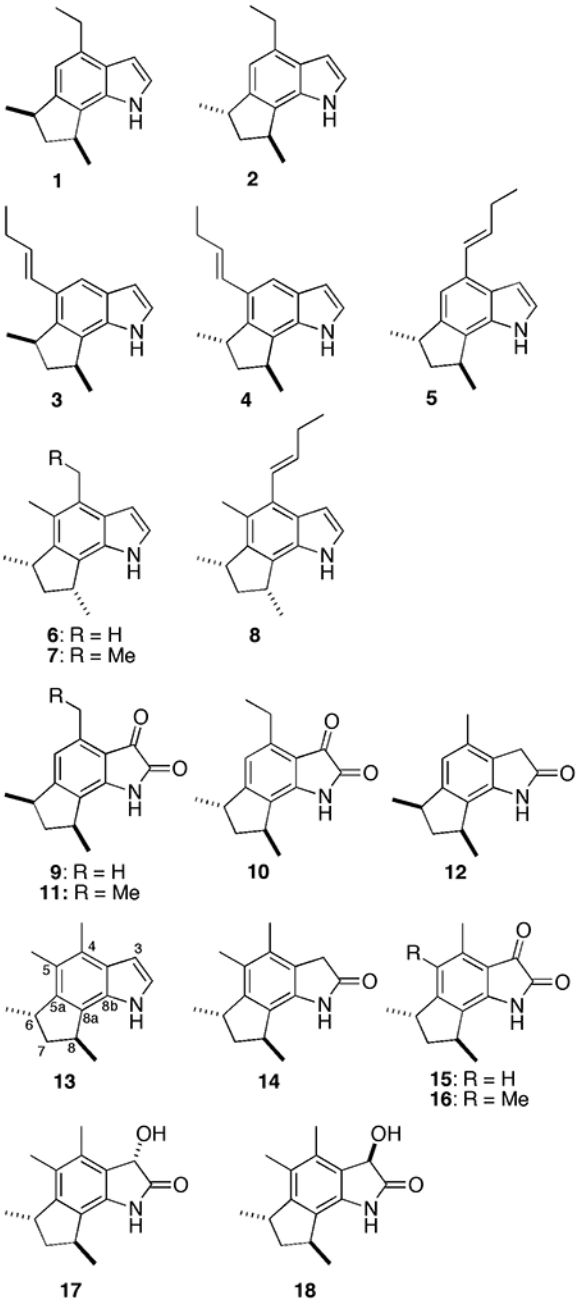

Aside from the above-referenced syntheses, the total syntheses of (+)-**1**,[10,11] (+)-**2**,[12] (±)-**1** and (±)-**2**,[11,13,14,15,16,17,18] (+)-**3**,[11] (±)-**3**,[13,19] and (±)-**6**–**8** have been achieved.[13,19,20] A formal synthesis of (±)-**3** has also been reported,[21] and all total syntheses of trikentrin-herbindole family, up to 2009, have been reviewed.[22]

In all likelihood, the biosynthesis of polyhalogenated indoles in red alga is linked to the enduring natural history of indole, indoxyl, indigo dye, and other indigoid compounds from plants of the genus *Indigofera* and, as shown through genetic and ecological studies, bacterial biosynthesis.[23] On the other hand, the origin of the sponge-derived 1,3-

dimethylcyclopenta[*g*]indoles must differ considerably from the latter. To date, no hypotheses for the origin of **1**–**12** have been advanced.

Here, we report the structures of new trikentrin-like natural products, (+)-*trans*-herbindole A (**13**) and trikentramides E-I (**14**–**18**), from *T. flabelliforme* collected in Exmouth Gulf. The absolute configurations of **13**–**18** were assigned from chiroptical comparisons with trikentrins and herbindoles, and exploitation of van't Hoff's principle of optical superposition,[24] and chemical correlation to derive a new mnemonic for absolute stereostructure of this family of compounds. Surprisingly, the structures of **13**–**18** uniformly exhibit a *trans* configuration for the fused 1,3-dimethylcyclopentane ring, in contrast with the (–)-*cis*-herbindoles (**6**–**8**) obtained from a specimen of *T. flabelliforme* collected in the same vicinity,[4] and are enantiomorphic with the latter. A unifying hypothesis is proposed that rationalizes the biogenesis of trikentrins, herbindoles, trikentramides and two related sponge-derived indoles from West African *Trikentrion loeve*.

Results and Discussion.

A MeOH extract of lyophilized *Trikentrion flabelliforme*, collected in Exmouth Gulf, Western Australia in 1993, was redissolved in MeOH-H_2O (9:1), and the solution was partitioned progressively against hexanes, CH_2Cl_2, and *n*-BuOH. The CH_2Cl_2-soluble 'fraction B', enriched in indoles (TLC spots stained bright fuschia with vanillin-H_2SO_4), was separated by gel filtration chromatography (Sephadex LH-20) and further purified by reversed-phase HPLC (C_{18}) to obtain pure **13** –**18**.

The simplest of the new compounds, *trans*-herbindole A (**13)**, $C_{15}H_{19}N$ (HRESITOFMS *m/z* 214.1592 $[M+H]^+$), when compared with *cis*-herbindole A (**6**), confirmed that **13** and **6** are constitutional isomers, but diastereomeric in the 1,3-dimethylcyclopentane ring. Compound **13** displayed a relatively featureless ^{1}H NMR spectrum ($CDCl_3$) consisting of signals for a *trans*-1,3-dimethylcyclopentane ring: two methyl doublets (δ_H 1.21, 3H, d, J = 6.6 Hz and δ_H 1.49, 3H, d, J = 7.2 Hz), two methines (δ_H 3.46, 1H, quintet, J = 7.2 Hz; δ_H 3.71, 1H, qdd, J = 7.2, 7.8, 9.6 Hz) and H_2-7, a diastereotopic methylene group (H-7α δ_H 2.10, 1H, ddd, J = 1.2, 7.5, 12.1 Hz and H-7β, δ_H 1.97, 1H, ddd, J = 7.2, 9.6, 12.1 Hz).[25] The relatively small separation in chemical shifts of the H_2-7 proton signals ($\Delta\delta$ = 0.13 ppm) is characteristic of *pseudo*-enantiotopic methylene protons in *trans*-1,3-dimethylcyclopenta[*g*]indole rings (e.g. enantiotopic CH_2 in *trans*-1,3-dimethylindane, Figure 1a), as opposed to the larger signal separation ($\Delta\delta$ >1.3 ppm) observed in the corresponding diastereotopic methylene of the *cis*-isomers.[5,9] A broad exchangeable singlet (δ 8.02, 1H, bs) was assigned to the indole NH. The remaining signals were pairs of aryl methyls (δ_H 2.35, 3H, s and δ_H 2.50, 3H, s), and pyrrole ring proton signals (δ_H 6.55, 1H, dd, J = 3.0, 2.4 Hz, and δ_H 7.14, 1H, t, J = 2.4 Hz). Comparisons of the ^{13}C NMR chemical shifts of **13** with those of **9**-**12**[9] and *cis*-herbindole A (**6**)[5]further supported a 4,5-dimethylindole structure.

Trikentramide E, $C_{15}H_{19}NO$, (**14**) is an oxindole; the higher homolog of **12**. The ^{13}C chemical shifts of **14** at C-2 (δ_C 177.7 Cq) and C-3 (δ_C 35.7, CH_2) compare well with those

of indolin-2-one,[26] but not indolin-3-one.[27] Again, the 1,3-dimethylindane ring is *trans*-substituted.

The formulas of trikentramides F (**15**, $C_{14}H_{15}NO_2$) and G (**16**, $C_{15}H_{17}NO_2$), with two oxygens, suggested homologous isatins, differing by substitution by Me at C-5 in **16**. The red-shifted long-wavelength band in the UV-vis spectrum of each compound [λ_{max} 326 ($\log_{10}$ 3.54)] was consistent with a substituted isatin (indolin-2,3-dione). The ^{13}C NMR spectra ($CDCl_3$) showed pairs of downfield signals attributed to the aryl ketone and lactam carbonyl groups, respectively [e.g. **16**, δ 183.2 (C-3), 160.2 (C-2)], matched those reported for the parent heterocycle, isatin (δ 184.5, 159.5, DMSO-d_6).[28] The ^{1}H NMR spectra of the two compounds appeared similar to those of **14** and supported the same *trans*-1,3-dimethylcyclopenta[*g*]indole ring. Full ^{1}H and ^{13}C NMR assignments (Tables 1 and 2) were secured through analysis of COSY, NOESY, HSQC and HMBC spectra (Figures 2 and 3).

The formula of isomeric dioxindoles (+)-trikentramides H (**17**) and (+)-I (**18**), $C_{15}H_{19}NO_2Na^+$ (HRESITOFMS *m/z* 268.1307 and *m/z* 268.1305, respectively $[M+Na]^+$) confirmed the two are formal reduction products of **16**. The ^{13}C chemical shifts of **18** at δ_C 178.9 (C-2) and 69.7 (C-3), which are consistent with those of 3-hydroxy-5-methyl-indolin-2-one,[30] verified the dioxindole arrangement of keto and hydroxymethine groups at C-2 and C-3, respectively.

Absolute configurations of **13–18** were assigned from analysis of the CD and $[\alpha]_D$ data, and comparisons with published chiroptical data of known compounds and DFT calculations of ECD. The simplest assignment, by comparisons of $[\alpha]_D$s (Table 3), is that of (+)-*trans*-herbindole A (**13**, $[\alpha]_D$ +29.0) which follows from its structural similarity to (+)-*trans*-trikentrin A (**2**, $[\alpha]_D$ +23.3) and the relative invariance of $[\alpha]_D$ in trikentrins and herbindoles A and B, whether substituted at C-4 or C-5 by H, Me or Et (Table 3); therefore, both compounds bear the same (6*S*,8*S*) configuration (see below for more discussion).This is not necessarily true of **3**–**5**, and **8**; the conjugated *E*-butenyl chain, which constitutes a substituted styrenyl chromophore, adds complexity to the $[\alpha]_D$ of these indoles and abrogates simple chiroptical comparisons.

The specific rotations of oxidized indoline analogs, trikentramides A-I, do not follow a simple pattern; the magnitude and sign vary with substitution and electronic properties in a complex manner. For example, the two isatins **15** and **16** differ only in a single Me group at C-5, but show $[\alpha]_D$s ~0 and –43.4, respectively. These are confoundingly different from **13** and **14** (+29 and +19.0, respectively). Moreover, the $[\alpha]_D$ of highly dextrorotatory **18** (+232) appears to be largely influenced by the stereocenter at C-3. Consequently, in order to make the stereoassignments of **15** and **16**, we first chose to assign **17** and **18** by ECD and chemically correlate them to other family members.

Assignment of absolute configuration of trikentramides H (**17**) and I (**18**), which are epimeric dioxindoles, rested upon interpretation of their corresponding ECD spectra (Figure 4). The ECD spectra of oxidized indoles **14**–**16** exhibited relatively weak Cotton effects (CEs), not unlike Natsume's observations of indoles **1**-**3**.[7] In contrast, the ECDs of **17** [λ 243 ($\Delta\varepsilon$ –7.4), 221 (+8.6)] and **18** [λ 243 ($\Delta\varepsilon$ +5.0), 224 (–5.6)] are virtual mirror images

dominated by relatively strong biphasic CEs that reveal a predominant influence of the C-3 stereocenter.

Asymmetric reductions of isatins to 3-hydroxoxindoles have been reported that provide comparison compounds for chiroptical assignments of **17** and **18**.[29,30,31]

For example, isatin undergoes enzyme-catalyzed reduction in the presence of a carbonyl reductase derived from *Candida parapsilosis* to give (+)-(*R*)-dioxindole in 21%ee.[31] (*R*)-5-Methyldioxindole (**19**, 38.5%ee), prepared by Sonderegger and coworkers using partial asymmetric hydrogenation of **20** (H_2, Pt supported on Al_2O_3-(–)-cinchonidine, Scheme 1), exhibited an ECD spectrum dominated by a negative Cotton effect (CE) (λ 237 nm, –41, arbitrary units of ellipticity) and a second CE of opposite sign at longer wavelength (λ 264, +12.5).[30] The authors calculated the ECD spectrum of **19** using time dependent DFT (b3pw91 and 6–31G(d, p) basis set[32]) and assigned their reduction product (*R*)-**19**. We repeated the reduction of **20** under non-asymmetric conditions (EtOH, $NaBH_4$) and resolved the product, (±)-**19**, by chiral phase HPLC (Phenomenex Lux 5U, Amylose 2) into (*S*)-**19** and (*R*)-**19** which, as expected, exhibited mirror image ECD spectra (see Supporting Information). The near identity of the ECD spectra of (*R*)-**19** and (+)-**18**, and the expected weaker dichroic contributions from the 1,3-dimethylcyclopentane in other trikentramides (Figure 4b,c), leads to the conclusion that the configuration of the natural products are (3*S*, 6*S*,8*S*)-**17** and (3*R*,6*S*,8*S*)-**18**.

Reduction of **16** (Scheme 2, $NaBH_4$, EtOH, rt) gave the C-3 epimeric dioxindoles **17** and **18**, identical with the natural products by HPLC retention times, ^{1}H NMR, $[\alpha]_D$ and ECD. In addition, a minor product, from over-reduction of intermediate **17**/**18** at the benzylic carbon, was recovered and shown to match (+)-trikentramide E (**14)** by HPLC retention time, ^{1}H NMR and ECD. Finally, oxidation of the indole (+)-**13** under the selective conditions recently reported by Wang and coworkers (I_2, *t*-BuOOH, DMSO, 80 ˚C, Scheme 2),[33] gave a product identical with natural (–)-**16** by MS, ^{1}H NMR, ECD and HPLC retention time. Thus, (+)-*trans*-herbindole A (**13**) is chemically correlated to (+)-**14**, (–)-**16**, (+)-**17** and (+)-**18** demonstrating that the dimethylcyclopentane ring is stereochemically uniform among these five natural products. Although we have no independent correlation of (+)-trikentramide E (**15**), it seems highly probable the configuration is the same as to its congeneric family members.[34]

The observed ECD spectra of **17** and **18** are the molar sum contributions of *independent* asymmetric perturbations to the benzenoid chromophore by the 1,3-dimethylcyclopentane group and the benzylic secondary OH group within their respective ‘first spheres of asymmetry’. The latter is a formal corollary of van’t Hoff’s principle of optical superposition,[24] which has been applied both to configurational assignments through deconvolution of both molar rotation [ϕ] and ECD ($\Delta\varepsilon$),[35] in combination with DFT calculations (e.g. CADPAC calculated $[\alpha]_D$ of (–)-1,3,5,7-tetramethyl-1,3-dihydroindol-2-one[35c]).

The largest contribution to both the $[\alpha]_D$ and CD in *trans*- and *cis*-fused trikentrin-type indoles appears to be the C-8 stereocenter. For example, both (+)-*ent*-*cis*-**6** and (+)-*trans*-**13**

have the same C-8 configuration and are dextrorotatory, although the magnitude of $[\alpha]_D$ of the former is almost twice that of the latter (Table 3). The presence of a C-5 Me group has little effect on $[\alpha]_D$; *trans*-(+)-**2** and (+)-**13** have almost the same specific rotation ($[\alpha]_D$ = +23.3 and +29.0, respectively). A brief conformational analysis of *cis* and *trans* herbindoles was carried out (MMFF94 and DFT) to derive their lowest energy conformations and frontier molecular orbitals. The conformation of the cyclopenta[*g*]indole ring in **13** (Figure 5) is distorted from an idealized C_2 conformation by torsional strain and steric repulsion between the N-H bond and the methyl group, and between the Me groups at C-5 and C-6. For example, the C-5–C-5a–C-6–C-6(Me) dihedral angle is $\theta = 52.1^\circ$, but the C-8b–C-8a–C-8–C-8(Me) dihedral angle is considerably larger, $\psi = 72.3^\circ$, but the 'unstrained' *trans*-1,3-dimethylindane ***i*** – Figure 1 – which freely inverts between the two degenerate C_2 conformers – displays $\theta = 40.1^\circ$; $\psi = 76.1^\circ$. In contrast, the cyclopentane ring of (+)-*cis*-herbindole A (*ent*-**6**) has an almost symmetric envelope conformation ($\theta = -53.2^\circ$, $\psi = 48.3^\circ$).

The major difference in frontier molecular orbitals of the delocalized π-system in 1,3-cyclopenta[*g*]indoles is the distortion of the LUMO by non-bonded interactions, particularly by the C-8 methyl group, which influences the rotational strength, and therefore ECD and $[\alpha]_D$, by altering molecular orbital symmetry properties. The influence of the C-8 stereocenter upon chiroptical properties is extrapolated into a simple stereochemical mnemonic (Figure 6): for trikentrin-herbindole like indoles, the absolute configuration at C-8 determines the sign of $[\alpha]_D$, whether the 1,3-dimethylcyclopentane ring is *cis*- or *trans*-fused. The exceptions are 1-butenyl substituted compounds (e.g. **3**) where contributions from the additional rotational strength of the styrenyl chromophore perturbs this simple rule. As the presence of C-4 or C-5 alkyl substituents (e.g. Me, Et) appear not to significantly change the relationship between sign of specific rotation and absolute configuration, we predict that hydrogenation of 1-butenyl to an *n*-butyl group, prior to measuring the $[\alpha]_D$, will restore the relationship; the products should conform to the mnemonic and allow stereoassignment.

The biosynthesis of most natural product indoles follows familiar routes. Free indole is oxidatively liberated from Trp by the action of a tryptophanase (L-Trp indole lyase). Certain bacteria are known to harbor the enzyme and, in combination with oxidases, could give rise to polyhalogenated indoles in *Rhodophycae*. In considering possible biosynthetic pathways that generate **1**–**18**, degradation of Trp seems unlikely; not only does C-3 of the indole ring lack a carbon substituent, but the introduction of the fused carbocyclic ring at C-5a,b and additional carbon substituents at C-4 and C-5 necessitates unwieldy complexity in this putative biogenesis. Consequently, alternative pathways must be considered. Alignment of the structures of two C-2 substitued indenyl-pyrrole metabolites, trikentramine (**21**)[36] and trikendiol (**22**)[37] (Figure 7, both isolated from West African *Trikentrion loeve*) with *cis*-trikentrin A (**1**) suggests a hypothesis: the trikentrin-herbindole family are of polyketide origin. Proline is oxidatively modified to the hypothetical pyrrole-2-carboxylic as a starter unit for ketide extensions by malonate (acetate) or methylmalonate (propionate).[38] In this scheme, the origin of the benzenoid ring differs slightly between two pathways, *a* and *b*. Because the C-C bond formation aligns carbons formally derived from the C=O group of the

ketide extender units, it is unlikely that cyclization proceeds by aldol/Claisen condensations familiar from the biosynthesis of aromatic Type II polyketides. The indane ring of trikentramine (pathway *a*) is mostly likely assembled after partial reductions and polyene electrocyclization reactions – possibly involving oxidative single electron transfer (SET)[39] – followed by aromatization to the benzene ring. For trikentrin-like secondary metabolites, (pathway *b*), similar reactions proceed, but for the fused indole ring we invoke a Friedel-Craft type intramolecular alkylation at C-3 (pyrrole numbering) of the electron-rich pyrrole ring for construction of the C-3b–C-4 bond. Indeed, Natsume exploited a similar reaction for the indole ring-closing steps in the total syntheses of **2**, **4**, and **5**.[6]

The hypothesis succinctly accounts for the location of substituents at C-4 and C-5, namely H, Me, Et or 1-butenyl, through chain extensions or termination of the polyketide chain by homologated malonate units. Subsequently, a manifold of oxidative reactions of the product indoles would generate **20** or, conversely, the oxindole, isatin, and dioxindole scaffolds found in trikentramides A–D (**9**-**12**) and E–I (**14**–**18**).

Conclusion.

Six new cyclopenta[*g*]indole natural products – *trans*-herbindole A (**13**) and trikentramides E-I (**14**–**18**) – were isolated from the sponge *Trikentrion flabelliforme* and their absolute stereostructures solved by integrated analysis of MS, NMR and ECD studies, in combination with calculated DFT, and chemical correlation. A simple mnemonic emerged from analysis of the chiroptical data that allows easy identification of absolute configuration of indoles and dioxindoles within the series.

EXPERIMENTAL SECTION

General Experimental Procedures.

Optical rotations were measured on a JASCO P-2000 at the D-double emission line of Na. UV-vis spectra were measured on a JASCO V-630, spectrometer. ECD spectra were measured on a JASCO J-810 spectropolarimeter in quartz cells (1 or 5 mm pathlength) at 23 ˚C. FTIR spectra were collected on thin film samples using a JASCO FTIR-4100 fitted with an ATR accessory (ZnSe plate). Inverse-detected 2D NMR spectra were measured on a JEOL ECA (500 MHz) spectrometer, equipped with a 5 mm $^{1}H\{^{13}C\}$ room temperature probe, or a Bruker Avance II (600 MHz) NMR spectrometer with a 1.7 mm $^{1}H\{^{13}C/^{15}N\}$ microcryoprobe. ^{13}C NMR spectra were measured on a Varian NMR spectrometer (125 MHz) equipped with a 5 mm Xsens $^{13}C\{^{1}H\}$ cryoprobe. NMR spectra were referenced to residual solvent signals, ($CDCl_3$, δ_H 7.26, δ_C 77.00 ppm). High-resolution ESITOF analyses were carried out on an Agilent 1200 HPLC coupled to an Agilent 6350 TOFMS at the Small Molecule MS Facility (UCSD). Low-resolution MS measurements were made using a Thermoelectron Surveyor UHPLC coupled to an MSD single-quadrupole detector. Preparative and analytical HPLC was performed on an Agilent 1100 HPLC, or a Jasco system comprising dual-pumps (PU-2086) and mixer, UV-vis detector (UV-2075) in tandem with an ELSD detector (Softa-A model 300).

Animal Material.

The sponge *T. flabelliforme* (93-07-076) was collected in Exmouth Gulf (800 m south of Bundegi Beach), Western Australia, in 1993 at a depth of –9 m using scuba. The sponge was an orange, pliable, ear-shaped specimen with a smooth surface that, with pressure, emitted a red exudate. Microscopic spicule analysis revealed the predominance of styles consistent with the species *T. flabelliforme*. A voucher sample of the sponge is archived at UC San Diego.

Extraction of Sponge and Isolation of (+)-*trans*-Herbindole A (13) and Trikentramides E-I (14–18).

Lyophilized *Trikentrion flabelliforme* (63.88 g dry wt) was extracted with CH_2Cl_2-MeOH (2 × 400 mL, 12 h), and the combined organic extracts were concentrated and dissolved in H_2O-MeOH (1:9, 400 mL) prior to repeated extraction with hexane (400 mL x 2). Concentration of the hexane-soluble layer gave Fraction A (1.4604 g). The aqueous-MeOH layer was adjusted to 2:3 H_2O-MeOH followed by extraction with CH_2Cl_2 (500 mL x 2) to yield Fraction B (0.6845 g). The aqueous layer was concentrated and extracted with *n*-BuOH (400 mL x 2) to yield the C layer (0.8460 g). The remaining aqueous layer was dried to yield Fraction D (1.7995 g). Fraction B, the TLC of which stained bright fuschia[40] with vanillin-H_2SO_4, was separated further by size exclusion chromatography (Sephadex LH-20, elution with MeOH) to give 10 fractions, which were pooled according to TLC (10% MeOH-CH_2Cl_2), UV-activity and staining with vanillin-H_2SO_4 in EtOH. Fractions 4 (0.0698 g) and 6 (0.0357 g) were further purified by reversed-phase HPLC (Phenomenex, Kinetex C_{18} column, 150 × 21.2 mm, linear gradient, initial conditions 75:25 H_2O-0.1% TFA-CH_3CN for three minutes, 30:70 for 17 minutes to 100% CH_3CN for the last 6 minutes, flow rate = 12 mL·min^{-1}) to give *trans*-herbindole A (**13**, 4.7 mg, 0.0074 % dry mass, t_R = 25.26 min), trikentramides F (**15**, 2.4 mg, 0.0038 % dry mass, t_R = 18.21 min), G (**16**, 5.5 mg, 0.0086 % dry mass, t_R = 19.62 min), H (**17**, 1.6 mg, 0.0025 % dry mass, t_R = 15.12 mim) and I (**18**, 2.8 mg, 0.004 % dry mass, t_R = 15.42 min). Pure trikentramide E (**14**, 1.8 mg, 0.0028 % dry mass, t_R = 21.32 min) was obtained after slightly different reversed-phase HPLC conditions (Phenomenex, Kinetex C_{18} column, 150 × 21.2 mm, linear gradient, initial conditions 75:25 H_2O-0.1% TFA-CH_3CN for three minutes, 30:70 for 21 minutes to 100% CH_3CN for the last 2 minutes, flow rate = 12 mL·min^{-1}).

(+)-trans-*Herbindole A (**13**):* Gray oil; UV (CH_3CN) λ_{max} 221 nm (logε 4.53), 271 (3.86); $[\alpha]_D^{23}$ +29 (*c* 0.24, $CHCl_3$); ECD (CH_3CN) λ 214 (Δε +5.3), 230 –7.3), 269 (–3.0), 294 (+0.66); FTIR (ATR, ZnSe plate) ν 3430, 2953, 1393, 1375, and 727 cm^{-1}; ^{1}H NMR and ^{13}C NMR ($CDCl_3$), Tables 1 and 2; HRESITOFMS *m/z* 214.1592 [M+H]+ (calcd for $C_{15}H_{20}N^+$ 214.1590).

*(+)-Trikentramide E (**14**)*[41]: pale orange solid; UV (CH_3CN) λ_{max} 204 nm (logε 4.10), 213 (4.08), 253 (3.63); $[\alpha]_D^{23}$ +19 (*c* 0.18, $CHCl_3$); ECD (CH_3CN) λ 215 (Δε –1.45); FTIR (ATR, ZnSe plate) ν 3206, 2948, 2871, 1670 (s), 1626 (s), and 711 cm^{-1}; ^{1}H NMR and ^{13}C NMR ($CDCl_3$), Tables 1 and 2; HRESITOFMS *m/z* 230.1534 $[M+H]^+$ (calcd for $C_{15}H_{20}NO^+$ 230.1539).

*Trikentramide F (**15**):* Dark yellow solid; UV (CH_3CN) λ_{max} 199 nm (logε 4.23), 218 (4.03), 245 (3.98), 326 (3.54); $[\alpha]_D^{23}$ ~0 (*c* 0.12, $CHCl_3$); ECD (CH_3CN) λ 210 (Δε +2.4), 214 (2.2), 252 (–0.7); FTIR (ATR, ZnSe plate) ν 3177, 2960, 2932, 1737 (s), 1726, 1638, 1390 and 1377 cm^{-1}; ^1H NMR and ^{13}C NMR ($CDCl_3$), Tables 1 and 2; HRESITOFMS *m/z* 230.1173 $[M+H]^+$ (calcd for $C_{14}H_{16}NO_2^+$ 230.1176).

*(–)-Trikentramide G (**16**):* Orange solid; UV (CH_3CN) λ_{max} 199 nm (logε 4.36), 218 (4.14), 249 (4.14), 328 (3.70); $[\alpha]_D^{23}$ –43 (*c* 0.55, $CHCl_3$); ECD (CH_3CN) λ 192 (Δε –2.2), 203 (–2.6), 221 (+4.9), 255 (+1.1); FTIR (ATR, ZnSe plate) ν 3311 (br), 2946, 2872, 1738 (s), 1725 (s), 1626, 1592, 1382 and 1344 cm^{-1}; ^1H NMR and ^{13}C NMR ($CDCl_3$), Tables 1 and 2; HRESITOFMS *m/z* 244.1331 $[M+H]^+$ (calcd for $C_{15}H_{18}NO_2^+$ 244.1332).

*(+)-Trikentramide H (**17**):* Pale yellow solid; UV (CH_3CN) λ_{max} 269 nm (logε 3.97), 221 (4.17); $[\alpha]_D^{23}$ +22.6 (*c* 0.053, $CHCl_3$); ECD (CH_3CN) λ 221 (Δε +8.6), 243 (–7.4), 272 (+0.6); FTIR (ATR, ZnSe plate) ν 3311 (br), 2957, 2928, 1715 (s), 1704 (s), 1633 and , 1203 and 727 cm^{-1}; ^1H NMR and ^{13}C NMR ($CDCl_3$), Tables 1 and 2; HRESITOFMS *m/z* 268.1309 $[M+Na]^+$ (calcd for $C_{15}H_{19}NO_2Na^+$ 268.1308).

*(+)-Trikentramide I (**18**):* Tan solid; UV (CH_3CN) λ_{max} 221 nm (logε 3.96), 252 (3.39); $[\alpha]_D^{23}$ +232 (*c* 0.093, $CHCl_3$); ECD (CH_3CN) λ 224 (*Δε* –5.6), 243 (+5.0); FTIR (ATR, ZnSe plate) ν 3397 (br), , 2958, 2925, 1681 (s), 1633 (s), 1447, 1204 1189, and 1138 cm^{-1}; ^1H NMR and ^{13}C NMR ($CDCl_3$), Tables 1 and 2; HRESITOFMS *m/z* 268.1305 $[M+Na]^+$ (calcd for $C_{15}H_{19}NO_2Na^+$ 268.1308).

Reduction of 5-Methylisatin – Dioxindoles (*S*)-19 and (*R*)-19.

Reduction of 5-methylisatin (**20**, 200 mg, 1.2 mmol) with $NaBH_4$ (was carried out according to the protocol described by Hara and coworkers.[42] The crude product was purified by silica flash chromatography (1:1 EtOAc/$CHCl_3$) to provide (±)-5-methyldioxindole [(±)-**19**] as a colorless solid, 101 mg (50%). UV-vis (CH_3CN) λ_{max} 209 nm (logε 4.11), 248 (3.65), 296 (2.88). LRMS *m/z* 164.20 $[M+H]^+$. The ^1H and ^{13}C NMR spectra of the product matched the literature values for (*R*)-**19**.[30]

A sample of (±)-**19** (~100 μg) was resolved by chiral reverse-phased HPLC (Lux 5U Amylose-2 column, 250 × 4.60 mm, isocratic conditions 2.5% *i*-PrOH-CH_3OH, flow rate = 1 mL·min^{-1}) to give the enantiomeric dioxindoles (*R*)-**19** (t_R = 4.68 min) and (*S*)-**19** (t_R = 5.52 min). (*S*)-**19**: ECD (2.5% *i*-PrOH-CH_3OH) λ 210 (Δε +54), 240 (–24.5), 267 (+7.4). (*R*)-**19**: λ 210 (Δε –54), 240 (+24.9), 267 (–7.0), [lit.[30] 237 (–41), 264 (+12.5), arbitrary units of ellipticity]. See Supporting Information for ECD spectra.

Reduction of (–)-Trikentramide G (16).

$NaBH_4$ (1.40 mg, 35.8 μmol) was added in portions to a solution of **16** (3.0 mg, 8.2 μmol) in anhydrous EtOH (1.0 mL) at room temperature. After 1 hr., the solution was diluted with H_2O (2.0 mL), acidified to pH ~ 6 with HCl (1N), and extracted with CH_2Cl_2 (2 × 2 mL). The organic layer was dried and the residue (5.2 mg) was purified by reversed-phase HPLC (Phenomenex, Kinetex C_{18} column, 150 × 21.2 mm, linear gradient, initial conditions 75:25 H_2O-0.1% TFA-CH_3CN for three minutes, 30:70 for 17 minutes to 100% CH_3CN for the

last 6 minutes, flow rate = 12 mL·min^{-1}) to give **14** (0.5 mg, 18%, t_R = 19.30 min), **17** (1.0 mg, 33%, t_R = 15.13 min) and **18** (1.2 mg, 40%, t_R = 15.43 min) with ECD and HPLC retention times identical with the natural products.

Oxidation of (+)-*trans*-Herbindole A (13) to (–)-Trikentramide G (16).

(+)-*trans*-Herbindole A (**13**) was oxidized according to the procedure of Wang and coworkers.[33] A solution of (+)-**13** (1.0 mg, 4.7 μmol) in DMSO (0.05 mL) was treated with a solution of iodine (1.4 mg, 5.6 μmol) and *t*-butyl hydroperoxide (70% w/v solution in H_2O, 3.0 μL, 23.4 μmol) in DMSO (0.50 mL) and heated to 80 ˚C with stirring for 18 h. The solution was cooled, quenched with aqueous $Na_2S_2O_3$ (5% w/v, 2.0 mL), extracted with EtOAc (3 × 1.0 mL) and purified by reversed-phase HPLC (Luna C_{18} column, 250 × 4.60 mm, linear gradient, initial conditions 65:35 H_2O-0.1% TFA-CH_3CN for three minutes, 30:70 for 20 minutes to 100% CH_3CN for the last 6 minutes, flow rate = 1.0 mL·min^{-1}) to give a product, as a yellow glass (0.5 mg, 44%) that was identical to natural (–)-trikentramide G (**16**) by MS, ^{1}H NMR, ECD and HPLC retention time.

Supplementary Material

Refer to Web version on PubMed Central for supplementary material.

ACKNOWLEDGEMENTS

We thank S. Taylor and D. Manker for assistance with sponge collections, and X. Cao (UCSD) for preliminary extractions and HPLC. We are grateful to S. Wang (Soochow University, PRC) for helpful advice on oxidations of indoles to isatins, Y. Su (UCSD) for HRMS data, and B. Duggan and A. Mrse (UCSD) for assistance with NMR measurements. The 500 MHz NMR spectrometer and the HPLC TOFMS were purchased with funding from the NSF (Chemical Research Instrument Fund, CHE0741968) and the NIH Shared Instrument Grant (S10RR025636) programs, respectively. This work was supported by a grant from NIH (R01 AI1007786).

References

(1). (a)Głowacki ED; Voss G; Leonat L; Irimia-Vladu M; Bauer S; Sariciftci NS Isr. J. Chem 2012, 52, 1–12.(b)Benkendorff K; McIver CM; Abbott CA Evid.-Based Complement Altern. Med 2011, 1–12. doi:10.1093/ecam/nep042(c)Baker JT Endeavour 1974, 33, 11–17.

(2). (a)Susse P; Krampe C Naturwissenschaften 1979, 66, 110.(b)Larsen S; Watjen F Acta Chem. Scand 1980, A34, 171–176.

(3). (a) Woolner VH; Jones CM; Field JJ; Fadzilah NH; Munkacsi AB; Miller JH; Keyzers RA; Northcote PT J. Nat. Prod 2016, 79, 463–469. [PubMed: 26756908] (b)Woolner VH PhD thesis, Victoria University of Wellington, 2017.

(4). Capon RJ; Macleod JK; Scammells PJ Tetrahedron 1986, 42, 6545–6550.

(5). Herb R; Carroll AR; Yoshida WY; Scheuer PJ; Paul VJ Tetrahedron 1990, 46, 3089–3092.

(6). (a) Muratake H; Natsume M Tetrahedron Lett. 1989, 30, 5771–5772.(b)Muratake H; Watanabe M; Goto K; Natsume M Tetrahedron 1990, 46, 4179–4192.(c)Muratake H; Seino T; Natsume M Tetrahedron Lett. 1993, 34, 4815–4818.

(7). Muratake H; Mikawa A; Natsume M Tetrahedron Lett. 1992, 33, 4595–4598.

(8). Lee M; Ikeda I; Kawabe T; Mori S; Kanematsu KJ Org. Chem 1996, 61, 3406–3416.

(9). Khokhar S; Feng Y; Campitelli MR; Quinn RJ; Hooper JNA; Ekins MG; Davis RA J. Nat. Prod 2013, 76, 2100–2105. [PubMed: 24188049]

(10). (a) Silva LF; Craveiro MV Org. Lett 2008, 10, 5417–5420. [PubMed: 18973334] (b)Tébéka IRM; Longato GB; Craveiro MV; de Carvalho JE; Ruiz ALTG; Silva LF Chem. Eur. J 2012, 18, 16890–16901. [PubMed: 23124578]

(11). Liu W; Lim HJ; RajanBabu TV J. Am. Chem. Soc 2012, 134, 5496–5499. [PubMed: 22394308]

(12). (a) Tébéka IRM; Longato GB; Craveiro MV; de Carvalho JE; Ruiz ALTG; Silva LF Chem. Eur. J 2012, 18, 16890–16901. [PubMed: 23124578] (b)Silva LF; Craveiro MV Org. Lett 2008, 10, 5417–5420. [PubMed: 18973334]

(13). Wiedenau P; Monse B; Blechert S Tetrahedron 1995, 51, 1167–1176.

(14). Huntley RJ; Funk RL Org. Lett 2006, 8, 3403–3406. [PubMed: 16836416]

(15). Leal RA; Bischof C; Lee YV; Sawano S; McAtee CC; Latimer LN; Russ ZN; Dueber JE; Yu J-Q; Sarpong R Angew. Chem. Int. Ed 2016, 55, 11824–11828.

(16). Jackson SK; Kerr MA J. Org. Chem 2007, 72, 1405–1411. [PubMed: 17256909]

(17). Macleod J; Monahan L Aust. J. Chem 1990, 43, 329–337.

(18). Boger DL; Zhang MJ Am. Chem. Soc 1991, 113, 4230–4234.

(19). Jackson SK; Banfield SC; Kerr MA Org. Lett 2005, 7, 1215–1218. [PubMed: 15787470]

(20). Chandrasoma N; Pathmanathan S; Buszek KR Tetrahedron Lett. 2015, 56, 3507–3510. [PubMed: 26516291]

(21). Karmakar R; Wang K-P; Yun SY; Mamidipalli P; Lee D Org. Biomol. Chem 2016, 14, 4782–4788. [PubMed: 27145857]

(22). Silva LF; Craveiro MV; Tébéka IR M. Tetrahedron 2010, 66, 3875–3895.

(23). (a)Ensley B; Ratzkin B; Osslund T; Simon M; Wackett L; Gibson D Science 1983, 222, 167–169. [PubMed: 6353574] (b)Gil-Turnes M; Hay M; Fenical W Science 1989, 246, 116–118. [PubMed: 2781297]

(24). van't Hoff JH Die Lagerung der Atome im Raume, Vieweg, Braunschweig 1908, ch. 8, pp. 95–97.

(25). Attempted deconvolution of the scalar couplings within the deceptively simple H-6 and H-8 methine multiplet signals in the 1H NMR of 13 has led to inconsistencies in literature assignments (Refs. 4, 5 and 9). Here, we rigorously assigned both H-6 and H-8 signals in 13 through J analysis and 1H NMR spectral simulation(Castillo AM; Patiny, L.; Wist J, J. Magn. Reson 2011, 209, 123–130. [PubMed: 21316274] See Supporting Information, Figure S28). In the 1H NMR spectra of 13, 14, 16–18, H-6 shows only zero or weak coupling to H-7α (J ~ 0–1.2 Hz), consistent with the ~90° dihedral angle for H-6-C-6-C-7-H-7α (θ = 87.6°, for example, see Figure 5a). The exception is 15 (J = 3.0 Hz), the only compound in this family that lacks a C-5 substituent, allowing relaxation of steric strain and slight alteration of the cyclopentane conformation.

(26). Gassman PG; Gilbert DP; Luh T-YJ Org. Chem 1977, 42, 1340–1344.

(27). Gaywood AP; McNab H Synthesis 2010, 8, 1361–1364.

(28). Panasenko AA; Caprosh AF; Radul OM; Rekhter MA Russ. Chem. Bull 1994, 43, 60–63.

(29). Birolli WG; Ferrreira IM; Jimenez DEQ; Silva BNM; Silva BV; Pinto AC; Porto AL M. J. Braz. Chem. Soc. 2017, 28, 1023–1029.

(30). Sonderegger OJ; Bürgi T; Limbach LK; Baiker AJ Mol. Catal. A-Chem. 2004, 217, 93–101.

(31). Hata H; Shimizu S; Hattori S; Yamada HJ Org. Chem 1990, 55, 4377.

(32). Frisch MJ; Trucks GW; Schlegel HB; Scuseria GE; Robb MA; Cheeseman JR; Zakrzewski VG; Montgomery JA; Stratmann RE; Burant JC; Dapprich S; Millam JM; Daniels AD; Kudin KN; Strain MC; Farkas O; Tomasi J; Barone V; Cossi M; Cammi R; Mennucci B; Pomelli C; Adamo C; Clifford S; Ochterski J; Petersson GA; Ayala PY; Cui Q; Morokuma K; Malick DK; Rabuck AD; Raghavachari K; Foresman JB; Cioslowski J; Ortiz JV; Baboul AG; Stefanov BB; Liu G; Liashenko A; Piskorz P; Komaromi I; Gomperts R; Martin RL; Fox DJ; Keith T; Al-Laham MA; Peng CY; Nanayakkara A; Gonzalez C; Challacombe M; Gill PMW; Johnson B; Chen W; Wong MW; Andres JL; Gonzalez C; Head-Gordon M; Replogle ES; Pople JA Gaussian98, A.7 Ed., Gaussian Inc., Pittsburgh, PA, 1998.

(33). Zi Y; Cai Z-J; Wang S-Y; Ji S-J Org. Lett 2014, 16, 3094–3097. [PubMed: 24850466]

(34). Another interpretation of the near-zero [α]D of 15 is that the compound is racemic rather than coincidentally non-rotatory at the D emission line of Na˚, and that the other members are partially racemic. Given that the matching magnitudes of the ECD spectra of semi-synthetic and natural 17 and 18, this possibility appears highly unlikely. It may be more than coincidental, that

5-butenyl-substituted iso-trans-trikentrin B (5), which like 15, has a trans-dimethylcyclopentane ring and lacks substitution at C-5, also exhibits an [α]D ~0. See Ref. 6c.

(35). (a) Perry TL; Dickerson A; Khan AA.; Kondru RK; Beratan DN; Wipf P; Kelly M; Hamann MT Tetrahedron 2001, 57, 1483–1487.(b)Kondru RK; Wipf P; Beratan DN J. Phys. Chem. A 1999, 103, 6603–6611.(c)Kondru RK; Chen CHT; Curran DP; Beratan DN; Wipf P Tetrahedron: Asymmetry 1999, 10, 4143–4150.(d)Kondru RK; Wipf P; Beratan DN Science 1998, 282, 2247–2250. [PubMed: 9856945] (e)Kondru RK; Lim S; Wipf P; Beratan DN Chirality 1997, 9, 469–477. [PubMed: 9329177] (f)Stout EP; Molinski TF Eur. Chem. J 2012, 5131–5135.(g)Molinski TF; Biegelmeyer R; Stout EP; Wang X; Frota MLC; Henriques AT J. Nat. Prod 2013, 76, 374–381. [PubMed: 23268569] (h)We note that molar rotations, [ϕ]D, are preferred for critical, quantitative comparisons (e.g. DFT calculated [ϕ]D), however, here we compare and discuss [α]D for two practical reasons: (1) Ours is a semi-quantitative comparison, only, and (2) the molecular masses of the molecules being compared (Table 3) – are similar, deviating from the average by less than ±14% – less, we believe, than the typical error for measurement of [α]D. Therefore, the ranges of magnitudes of [ϕ]D and [α]D are about the same (see Table S3), but the measurement and reporting of the latter is more conventional and familiar to organic chemists.

(36). Aknin M; Miralles J; Kornprobst J-M; Faure R; Gaydou E-M; Boury-Esnault N; Kato Y; Clardy J Tetrahedron Lett. 1990, 31, 2979–2982.

(37). Loukaci A; Guyot M Tetrahedron Lett. 1994, 35, 6869–6872.

38). Chan YA; Podevels AM; Kevany BM; Thomas MG Nat. Prod. Rep 2009, 26, 90–114. [PubMed: 19374124]

(39). (a) Stout EP; Wang Y-G; Romo D; Molinski TF Angew. Chem. Intl. Ed 2012, 51, 4877–4881. (b)Stout EP; Morinaka BI; Wang Y-G.; Romo D; Molinski TF J. Nat. Prod 2012, 75, 527–530. [PubMed: 22455452]

(40). This color was associated solely with the presence (+)-trans-herbindole A (13) and may be a general property of trikentins-herbindoles.

(41). Given the age (24 years) of our specimen of Trikentrion flabelliforme, we are cogniscent of the possibility that all trikentramides may be products of autoxidation of trikentrins or herbindoles. Quinn and coworkers (Ref. 9) isolated trikentramides A-D from a specimen of an age only slightly younger than ours.

(42). Usami N; Kitahara K; Ishikura S; Nagano M; Sakai S; Hara A Eur. J. Biochem 2001, 268, 5755–5763. [PubMed: 11722560]

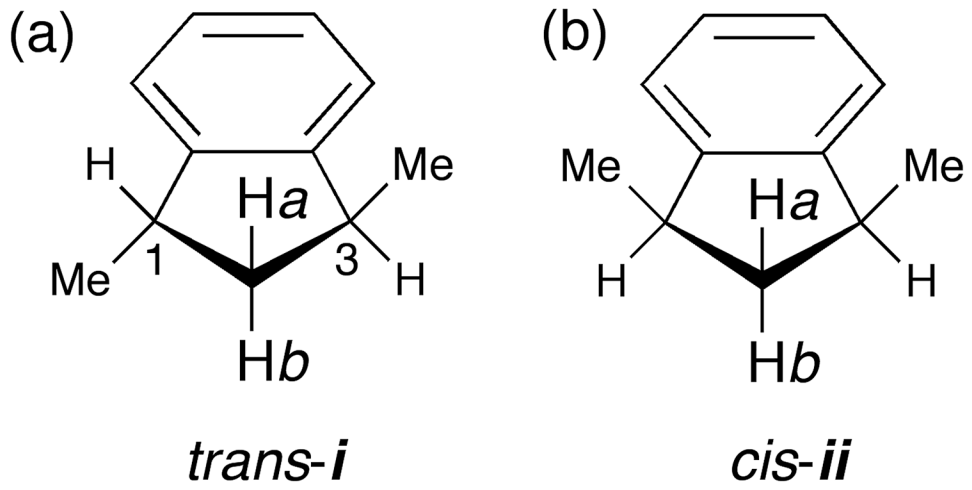

trans-***i*** *cis*-***ii***

Figure 1.

Stereotopicity of the CH_2 group in *trans*- and *cis*-1,3-dimethylcyclopentanobenzene (1,3-dimethylindane). (a) enantiotopic (b) diastereotopic.

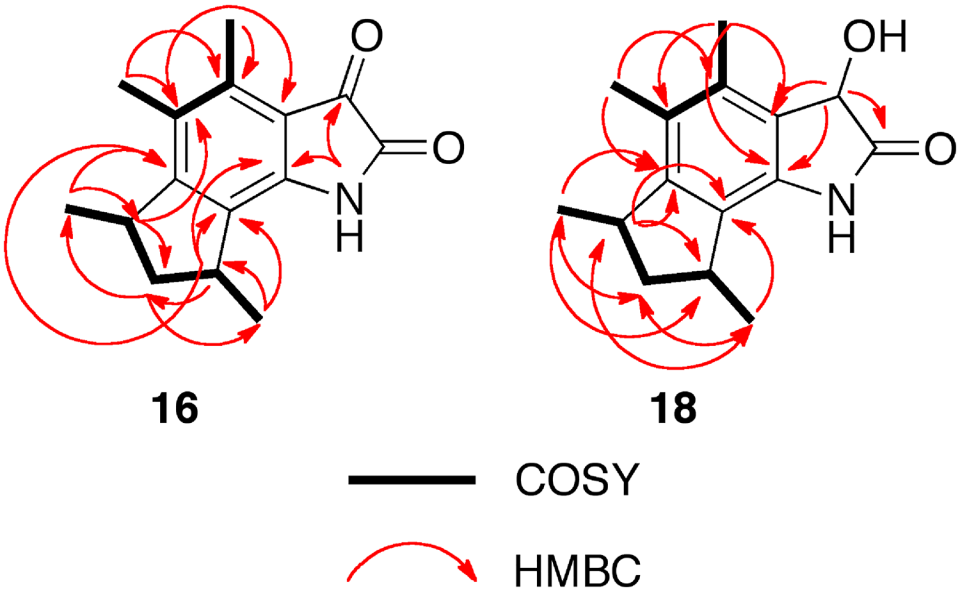

Figure 2.
COSY and HMBC correlations of (–)-trikentramide G (**16**) and (+)-trikentramide I (**18**) (500 MHz, $CDCl_3$).

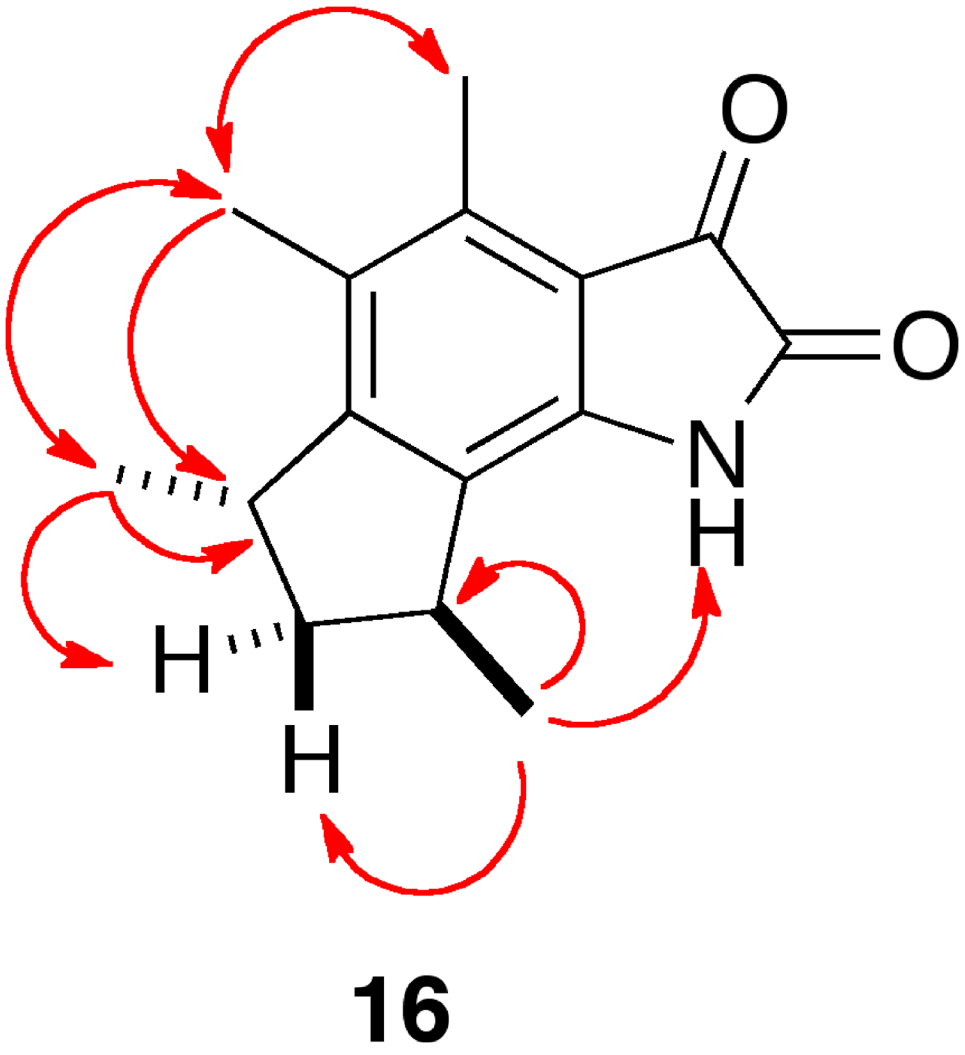

Figure 3.
NOESY correlations of (–)-trikentramide G (**16**) (600 MHz, $CDCl_3$).

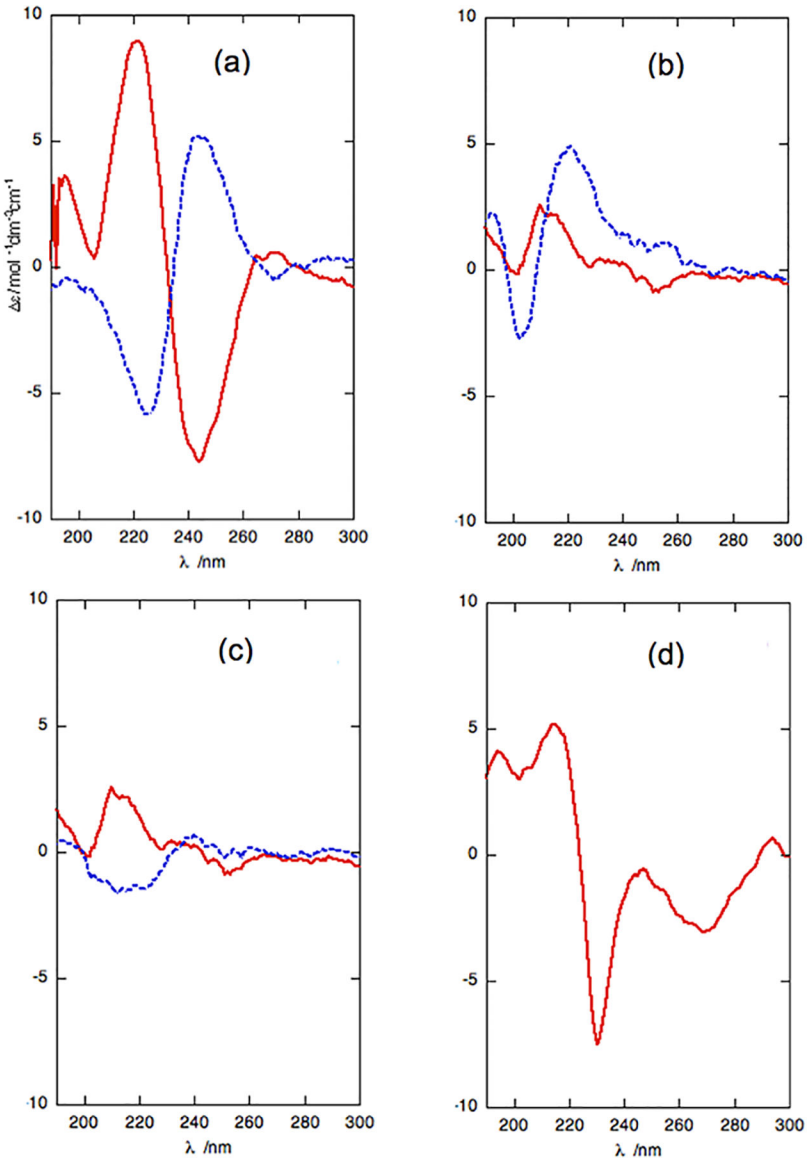

Figure 4.

ECD spectra (CH_3CN, 23 ˚C) of (a) trikentramides H [(+)-**17**] and I [(+)-**18**], dash). (b) trikentramides F [**15**] and G [(–)-**16**, dash]. (c) trikentramides F [(–)-**16**] and E [(+)-**14**, dash]. (d) *trans*-herbindole A [(+)-**13**].

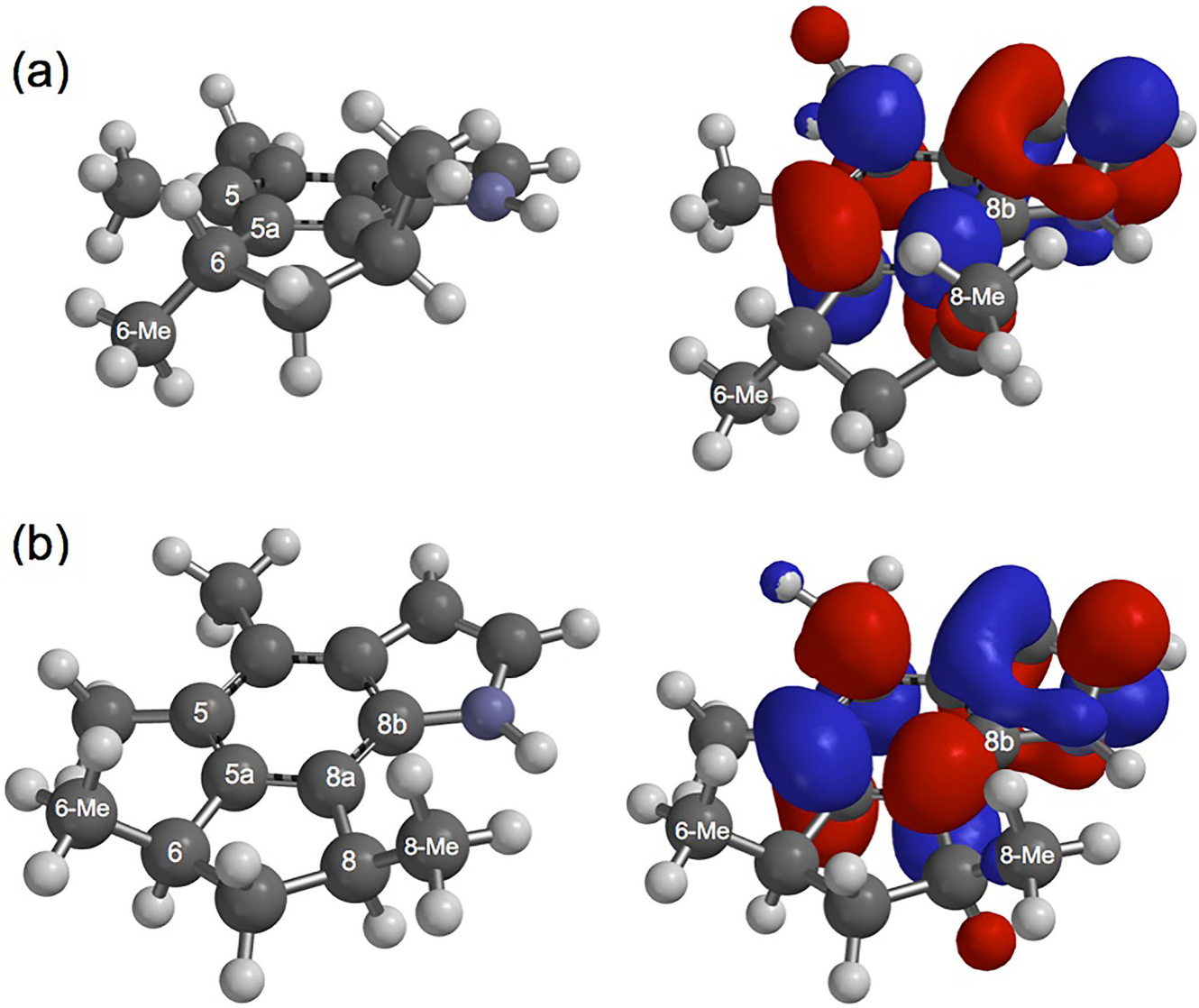

Figure 5.

Energy minimized geometries (MMFF) and DFT calculated (ωB97X-D 6–31G*) LUMO of (a) (+)-*trans*-herbindole A (**13**) and (b) (+)-*cis*-herbindole A (*ent*-**6**). Conformational searching returned only one conformation for **6** or **13**.

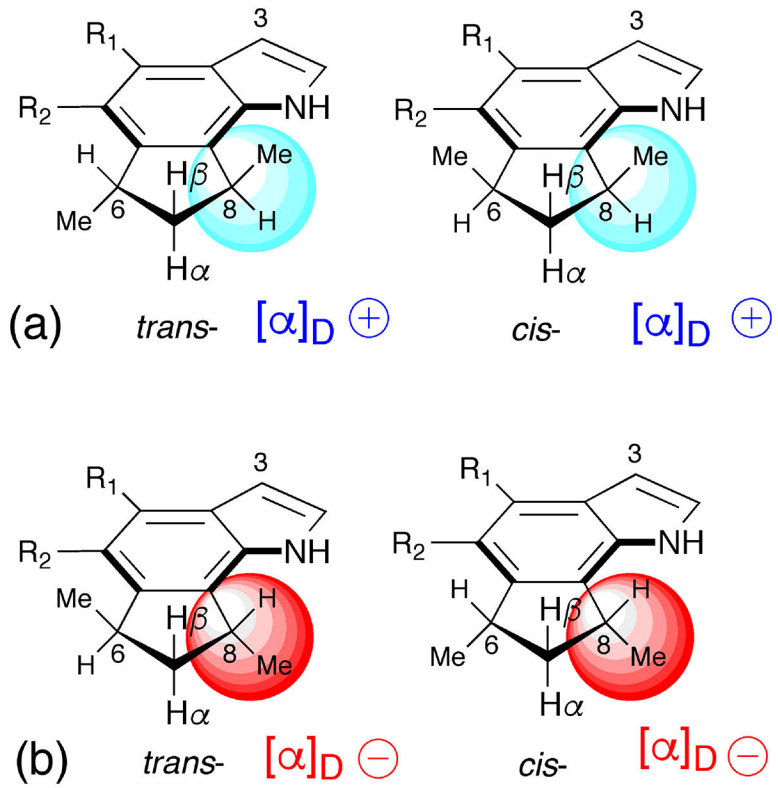

Figure 6.

Chiroptical mnemonic for assignment of absolute stereostructures of trikentrins and herbindoles (a) *trans*- and *cis*-8*S* (b) *trans*- and *cis*-8*R* (R_1, R_2 = H, alkyl, but ≠ 1-alkenyl)

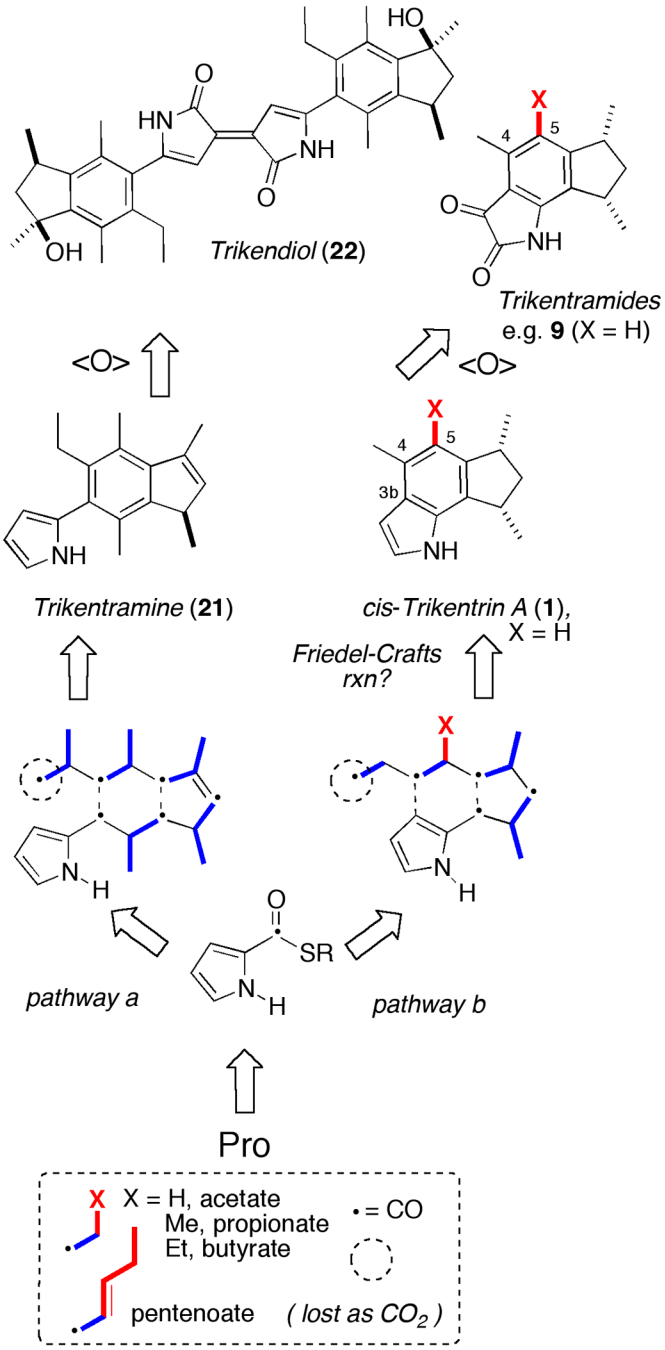

Figure 7.

Hypothesis for the biogenesis of trikentrin-like natural products, including *cis*-trikentrin A (**1**), trikentramine (**21**) and trikendiol (**22**).

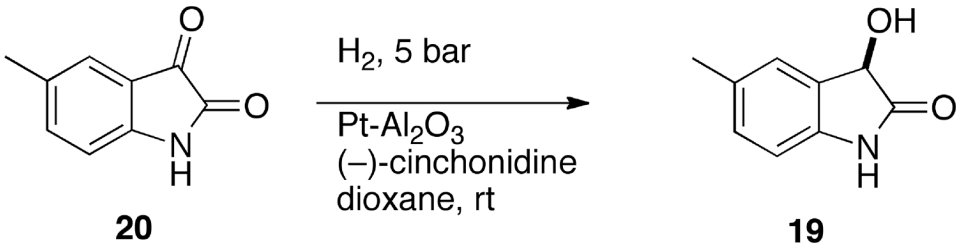

Scheme 1.

Partial asymmetric hydrogenation of 5-methylisatin. See Ref. 30 and Supporting Information for ECD.

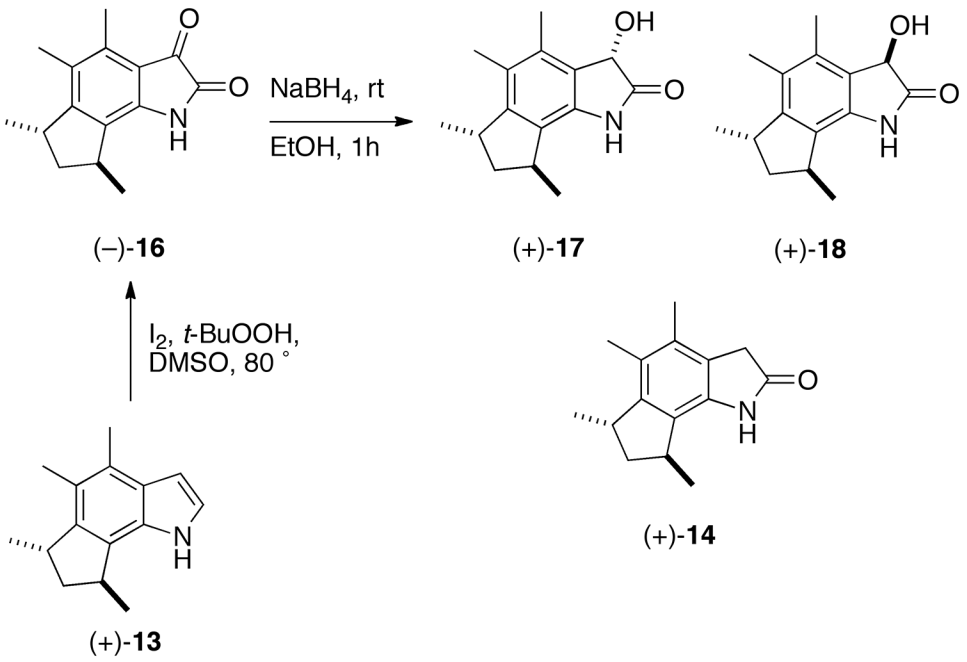

Scheme 2.
Chemical interconversions of (+)-**13** with (+)-**14**, (–)-**16**, (+)-**17** and (+)-**18**.

Table 1.

^{1}H NMR Data (δ, mult)[a] for **13**–**18**.

#	13	14	15	16	17	18
NH	8.03, bs	7.97, bs	8.80, bs	8.96, bs	7.99, bs	8.21, bs
2	7.14, t, 2.4					
3	6.55, dd (2.4, 3.0)	3.40, s			4.98, s	4.99, s
4						
5			6.68, s			
6	3.46, quin[b] (7.2)	3.31, quin[b] (7.2)	3.27, m[c]	3.29, quin[b] (7.2, 0.9)	3.27, quin[b] (7.2)	3.30, m[c]
7α	2.10, ddd, (1.2, 7.5, 12.1)	2.01, ddd, (1.2, 7.8, 12.3)	2.02, ddd, (3.0, 7.8, 12.6)	2.04, ddd, (1.5, 8.2, 12.6)	1.97, dd, (7.8, 12.6)	1.96, bdd[d], (7.8, 12.6)
7β	1.97, ddd, (7.2, 9.6, 12.1)	1.83, ddd, (7.2, 9.9, 12.3)	1.91, dt, (8.4, 12.6)	1.85, ddd, (7.2, 9.6, 12.6)	1.79, dt, (9.0, 12.6)	1.79, m
8	3.71, qdd, (7.2, 7.5, 9.6)	3.43, qdd, (6.6, 7.8, 9.9)	3.31, m[c]	3.44, qdd, (7.2, 8.2, 9.6)	3.37, m	3.40, m[c]
4-Me	2.50, s	2.18, s	2.55, s	2.49, s	2.28, s	2.28, s
5-Me	2.35, s	2.14, s		2.14, s	2.15, s	2.15, s
6-Me	1.21, d, (6.6)	1.13, d, (6.6)	1.26, d, (7.2)	1.14, d, (7.2)	1.12, d, (7.2)	1.07, d, (7.2)
8-Me	1.49, d, (7.2)	1.32, d, (6.6)	1.23, d, (6.6)	1.36, d, (7.2)	1.27, d, (6.0)	1.25, d, (6.6)

[a] 600 MHz, $CDCl_3$.

[b] quin = quintet.

[c] overlap.

[d] bdd = broad doublet of doublets.

Table 2.

^{13}C NMR Data (δ, mult)[a] for **13**–**18** ($CDCl_3$, 125 MHz).

#	13	14	15	16	17	18
2	122.9, CH	177.7, C	160.3, C	160.2, C	178.5, C	178.9, C
3	101.6, CH	35.7, CH_2	*b*	183.2, C	69.7, CH	69.7, CH
3a	126.3, C	123.2, C	115.2, C	115.7, C	124.1, C	124.1, C
4	128.1, C	135.2, C	140.9, C	139.9, C	134.6, C	134.4, C
5	123.1, C	125.9, C	121.0, C	127.0, C	127.1, C	127.3, C
5a	125.7, C	148.7, C	161.4, C	160.6, C	150.9, C	150.8, C
6	38.4, CH	37.9, CH	38.5, CH	38.8, CH	37.9, CH	38.0, CH
7	43.9, CH_2	43.8, CH_2	43.0, CH_2	43.2, CH_2	43.8, CH_2	43.7, CH_2
8	36.5, CH	35.4, CH	34.6, CH	35.2, CH	35.6, CH	35.5, CH
8a	143.0, C	125.3, C	128.9, C	128.4, C	125.7, C	126.0, C
8b	130.8, C	131.5, C	144.5, C	142.8, C	134.3, C	134.1, C
4-Me	15.7, CH_3	16.1, CH_3	18.5, CH_3	14.5, CH_3	15.4, CH_3	15.4, CH_3
5-Me	15.2, CH_3	16.1, CH_3	–	13.4, CH_3	14.9, CH_3	14.9, CH_3
6-Me	20.4, CH_3	19.7, CH_3	19.3, CH_3	19.5, CH_3	19.8, CH_3	19.6, CH_3
8-Me	20.7, CH_3	20.1, CH_3	19.8, CH_3	19.6, CH_3	20.0, CH_3	19.9, CH_3

[a]Multiplicities determined from edited HSQC, or comparisons with **9**–**12**. MHz (Ref. 9).

[b]Signal not observed.

Table 3.

$[\alpha]_D$ for Natural and Synthetic Trikentrins, Herbindoles and Trikentramides.

Config.	Cmpd.	Source[a]	$[\alpha]_D$[b]	Ref.
	(+)-**1**	N	+48[c]	4
	(+)-**1**	S	+49	11
ent-	(−)-**1**	S	−68.6	6a,b
	(+)-**2**	N	+23.3[d]	4
	(+)-**2**	S	+24	6c
	(+)-**2**	S	+24	10b
ent-	(−)-**2**	S	−26.8	6a,b
	(+)-**3**	S	+102	6c
	(+)-**3**	S	+100.2	8
	(+)-**3**	S	+101	11
	(−)-**4**	N	−13[e]	4
ent-	(+)-**4**	S	+24	6c
	5	S	~0	6c
	(−)-**6**	N	−62	7
ent-	(+)-**6**	S	+56.9	7
ent-	(+)-**7**	S	+51.2	6a
ent-	(+)-**8**	S	+19.9	7
	(+)-**9**	N	+40.7	9
	(+)-**11**	N	+42.2	9
	(+)-**12**	N	+50.0	9
	(+)-**13**	N	+29.0	*f*
	(+)-**14**	N	+19.0	*f*
	15	N	~0	*f*
	(−)-**16**	N	−43.4	*f*
	(+)-**17**	N	+22.6	*f*
	(+)-**18**	N	+231.5	*f*

[a] N = natural; S = synthetic.

[b] All measurements were made on solutions in $CHCl_3$ and, aside from the noted exceptions, within the concentration range *c*. ~0.027 – 0.50 g/100 cm^3.

[c] *c* = 2.47.

[d] *c* = 1.0.

[e] *c* = 1.97.

[f] This work.